Interplay of the Main Chain, Chiral Side Chains, and Solvent in Conformational Transitions: Poly{[(*R*)-3,7-dimethyloctyl]-[(*S*)-3-methylpentyl]silylene}

Akio Teramoto,*,†,∥ Ken Terao,†,∥,⊥ Yoshimi Terao,†,∥ Naotake Nakamura,†,∥ Takahiro Sato,‡,∥ and Michiya Fujiki§,∥

Contribution from the Research Organization of Science and Engineering and Faculty of Science and Engineering, Ritsumeikan University, 1-1-1 Nojihigashi, Kusatsu 525-8577, Japan, Department of Macromolecular Science, Osaka University, 1-1 Machikaneyama-cho, Toyonaka 560-0043, Japan, NTT Basic Research Laboratories, 3-1 Wakamiya, Morinosato, Atsugi 243-0198, Japan, and CREST-JST (Japan Science and Technology Corporation), 4-1-8 Honcho, Kawaguchi, Saitama 332-0012, Japan

Received June 25, 2001

Abstract: Light scattering, sedimentation equilibrium, viscosity, circular dichroism (CD), and UV absorption (UV) measurements were made on dilute solutions of poly{[(*R*)-3,7-dimethyloctyl]-[(*S*)-3-methylpentyl]silylene} (PRS) as functions of molecular weight. From light scattering and viscosity data, PRS is found to be a very stiff polymer of persistence length q as large as 103 nm at 25 °C, essentially a 7_3 helix found in the solid state; q increases only gradually with lowering temperature between −15 and 25 °C. The CD data show that PRS undergoes a conformational transition around 3 °C in isooctane (transition temperature T_c). The CD signal is largely positive at low temperatures, passes through zero at T_c, and becomes largely negative at higher temperatures; T_c is independent of sample's chain length N. This is a highly cooperative helix (M)-to-helix (P) transition depending remarkably on N, as PRS is substantially rodlike. The CD data are converted to the fraction f_P of P helix as a function of N and analyzed successfully by a statistical mechanical theory based on a helix reversal model, where a polymer chain consists of M and P helices intervened by helix reversals, with the result that the free energy difference ΔG_h between P and M shows a temperature dependence similar to that of $2f_P - 1$, whereas the helix reversal energy is substantially constant at 1.2×10^4 J mol^{-1}; the latter value means that the helix reversal occurs only once in 100 Si units or less. This ΔG_h change and solvent dependence of T_c are explained by a double-well potential for the rotation about Si−Si bonds, which incorporates into ΔG_h the solvent interactions with the helical grooves of side chains surrounding the main chain. Detailed features of UV absorption spectra at different temperature and molecular weights are also presented.

Introduction

There are a number of linear polymers capable of forming helical conformations and undergoing a thermal and/or solvent-induced transition from one conformation to another, always containing one helical conformation, for example, helix to random coil. Indeed, the helix is one of the most important conformations common to biopolymers and synthetic polymers.[1,2] Examples of such polymers are polypeptides,[3−5] polyisocyanates,[6−8] polysilylenes,[9−12] polyacetylenes,[13] and so forth. This transition is unique for its molecular-weight dependence, and theoretically, all these polymers are regarded as linear cooperative systems whose molecular-weight dependent conformations are formulated on the basis of a linear Ising model.[1,2] On the other hand, different polymers and solvents show different transition curves, and chemistry plays a crucial role. In other words, here is an interesting interplay between chemistry and physics; explicitly stated, the local or microscopic

† Ritsumeikan University.
‡ Osaka University.
§ NTT Basic Research Laboratories.
∥ CREST-JST.
⊥ Present Address: Department of Biological and Chemical Engineering, Faculty of Engineering, Gunma University, Kiryu 376-8515, Japan.

(1) Teramoto, A. *Prog. Polym. Sci.* **2001**, *26*, 667−720.
(2) Green, M. M. A Model for How Polymers Amplify Chirality. In *Circular Dichroism Principles and Applications*, 2nd ed.; Berova, N., Nakanishi, K., Woody, R. W., Eds.; Wiley-VCH: New York, 2000; Chapter 17.
(3) a. Teramoto, A.; Fujita, H. *Adv. Polym. Sci.* **1975**, *18*, 65−149. b. Teramoto, A.; Fujita, H. *J. Macromol. Sci., Rev. Macromol. Chem.* **1976**, *C15*, 165−278.
(4) Toriumi, H.; Saso, N.; Yasumoto, Y.; Sasaki, S.; Uematsu, I. *Polym. J.* **1979**, *17*, 977−981.
(5) Watanabe, J.; Okamoto, S.; Satoh, K.; Sakajiri, K.; Furuya, H.; Abe, A. *Macromolecules* **1996**, *29*, 7084−7088.
(6) a. Lifson, S.; Andreola, C.; Peterson, N. C.; Green, M. M. *J. Am. Chem. Soc.* **1989**, *111*, 8850−8858. b. Green, M. M.; Lifson, S.; Teramoto, A. *Chirality* **1991**, *3*, 285−291. c. Gu, H.; Nakamura, Y.; Teramoto, A.; Green, M. M.; Andreola, C.; Peterson, N. C.; Lifson, S. *Macromolecules* **1995**, *28*, 1016−1024. d. Green, M. M.; Peterson, N. C.; Sato, T.; Teramoto, A.; Lifson, S. *Science* **1995**, *268*, 1860−1866. e. Okamoto, N.; Mukaida, F.; Gu, H.; Nakamura, Y.; Teramoto, A.; Green, M. M.; Andreola, C.; Peterson, N. C.; Lifson, S. *Macromolecules* **1996**, *29*, 2878−2884. f. Gu, H.; Sato, T.; Teramoto, A.; Varichon, L.; Green, M. M. *Polym. J.* **1997**, *29*, 77−84. g. Gu, H.; Nakamura, Y.; Sato, T.; Teramoto, A.; Green, M. M.; Jha, S. K.; Andreola, C.; Reidy, M. P. *Macromolecules* **1998**, *31*, 6362−6368. h. Jha, S. K.; Cheon, K. S.; Green, M. M.; Selinger, J. V. *J. Am. Chem. Soc.* **1999**, *121*, 1665−1673. i. Gu, H.; Nakamura, Y.; Sato, T.; Teramoto, A.; Green, M. M.; Andreola, C. *Polymer* **1999**, *40*, 849−856. j. Li, J.; Schuster, G. B.; Cheon, K. S.; Green, M. M.; Selinger, J. V. *J. Am. Chem. Soc.* **2000**, *122*, 2603−2612.
(7) Maxein, G.; Zental, R. *Macromolecules* **1995**, *28*, 8438−8440.
(8) a. Maeda, K.; Okamoto, Y. *Macromolecules* **1998**, *31*, 5164−5166. b. Maeda, K.; Okamoto, Y. *Macromolecules* **1999**, *32*, 974−980. c. Hino, K.; Maeda, K.; Okamoto, Y. *J. Phys. Org. Chem.* **2000**, *13*, 361−367.

10.1021/ja011550f CCC: $20.00 © 2001 American Chemical Society
Published on Web 11/14/2001

chain structure of a polymer, which is responsible for chemical properties such as UV absorption, circular dichroism, and so forth, controls its global chain conformation or stiffness. Currently, we are particularly interested in conjugating polymers such as polyisocyanates[1,6] and polysilylenes,[12] whose conformations in dilute solution are helical and undergo transitions between left-handed and right-handed helices.

Green, Teramoto, and collaborators[1,2,6] studied the optical activity of chiral and achiral polyisocyanates in great detail and showed that they are analyzed quantitatively by a statistical theory proposed by Lifson et al.[6a] based on the helix reversal model, where a polymer chain consists of an alternating sequence of left-handed (M) and right-handed (P) helices intervened by helix reversal units. This theory contains two basic parameters, the free energy difference $2\Delta G_h = G_M - G_P$ between the M and P units and the energy ΔG_r for the helix reversal unit measured from the average of G_M and G_P, where G_M and G_P are the free energies in the M and P helices. It should be noted that the theory implicitly assumes that both terminal units can take the M and P conformations with equal probability. We have recently presented CD (circular dichroism) data for poly{*n*-hexyl-[(*S*)-3-methylpentyl]silylene} (PH3MPS, Chart 1), which change remarkably with temperature and molecular weight, and successfully analyzed them by fitting to the theory in a similar way.[12c] There is another interesting aspect of conjugating polymers: CD changes sign during the transition with temperature and/or solvent, which is interpreted to be due to a helix−helix transition. However, there is no experimental report as to the molecular-weight dependence of transition temperature T_c, which is a key factor for elucidating detailed molecular mechanisms, as the above theory predicts the dependence of T_c on molecular weight. In this connection, some chiral polysilylenes[11h,11i,11m] and other polymers[4,8] are shown to exhibit such CD sign changes in thermal transitions, but the molecular-weight independence of T_c has not been reported. Therefore, we have studied poly{[(*R*)-3,7-dimethyloctyl]-[(*S*)-3-methylpentyl]silylene} (PRS, Chart 1) in dilute solution by light scattering, sedimentation equilibrium, viscosity, and circular dichroism and analyzed the CD data to find that this is the first polymer to exhibit the predicted sign reversal. From the analysis of the molecular-weight dependence of CD, PRS is shown to undergo *a helix-to-helix transition* with helix reversals accompanying no *transition of global conformation or stiffness*; that is, it is not a transition of the helix-to-coil type as often proposed for thermochromism.[9] This paper reports experimental results and theoretical analysis in detail. The thermal transition of PRS depending remarkably on solvent is well described on the basis of a double-well potential for the internal rotation about Si−Si bonds of the main chain, which reflects the chemical structures of both the side chains and solvent. This transition arises from a fine chemical structure interplay of the main chain, chiral side chains, and solvent. The estimated values of the theoretical parameters ΔG_h and ΔG_r are discussed in connection with the chemical structures concerned, or alternatively, the chemical structures may be used for predicting the local and global conformations and functions of the polymer. The strategy used in the present study is not limited to our particular polysilylenes but is applicable to other polymers undergoing conformational transitions and will provide a novel means of predicting and designing polymers of desired conformational characteristics.

Chart 1

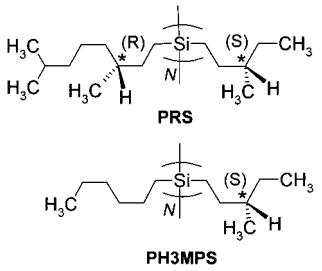

Experimental Section

A PRS sample synthesized by the procedure reported elsewhere[11m] was separated into many fractions by gel permeation chromatography (GPC) to obtain seven samples of different molecular weights RS-2 to RS-8. Sedimentation equilibrium experiments were made on four lower molecular weight fractions on a Beckman Optima XL-1 ultracentrifuge to determine the equilibrium concentration profiles in isooctane at 25 °C in the cell. Light scattering intensities were measured for three samples R-2 to R-4 in isooctane at 25 °C on a DAWN DSP light-scattering photometer. Zero-shear intrinsic viscosities $[\eta]$ in isooctane at 25 °C and the Huggins coefficient k' were determined using a four-bulb viscometer or a conventional viscometer of Ubbelohde type. UV absorption and CD measurements for seven samples RS-2 to RS-8 in isooctane at temperatures between −75 °C and 80 °C were made on a JASCO J700 circular dichroism spectrophotometer. It was confirmed that there was no photodegradation of the samples during these measurements. For the experimental details and data processing, consult ref 12b,c and the Supporting Information.

Experimental Results

Molecular Weight and Dimensional and Hydrodynamic Properties. Sedimentation equilibrium measurements yielded the equilibrium concentration profiles in the centrifuge cell, from which two apparent molecular weights M_{app} and Q were determined as functions of the average concentration ($\bar{c}$). M_{app}^{-1} and Q plotted against ($\bar{c}$) formed straight lines, whose ordinate intercept and slopes allowed us to determine the weight-average molecular weight M_W, the second virial coefficient A_2, and the *z*-average molecular weight M_z.[12b,c] On the other hand, light scattering measurements yielded the Rayleigh ratio R_θ as a function of the mass concentration c and the scattering angle θ. M_W, A_2, and *z*-average mean-square radius of gyration $\langle S^2 \rangle_z$

(9) a. West, R. *J. Organomet. Chem.* **1986**, *300*, 327−346. b. Miller, R. D.; Michl, J. *Chem. Rev.* **1989**, *89*, 1359−1410. c. Michl, J.; West, R. Electronic Structure and Spectroscopy of Polysilylenes. In *Silicon-Based Polymers*; Chojnowski, J., Jones, R. G., Ando, W., Eds.; Kluwer: Dordrecht, The Netherlands, 2000.

(10) Maeda, K.; Shimizu, K.; Azumi, T.; Yoshida, M.; Sakamoto, K.; Sakurai, H. *J. Phys. Chem.* **1993**, *97*, 12144−12146.

(11) a. Fujiki, M. *J. Am. Chem. Soc.* **1994**, *116*, 6017−6018. b. Fujiki, M. *J. Am. Chem. Soc.* **1994**, *116*, 11976−11981. c. Yuan, C.-H.; Hoshino, S.; Toyoda, S.; Suzuki, H.; Fujiki, M.; Matsumoto, N. *Appl. Phys. Lett.* **1997**, *71*, 3326−3328. d. Fujiki, M.; Toyoda, S.; Yuan, C.-H.; Takigawa, H. *Chirality* **1998**, *10*, 667−675. e. Toyoda, S.; Fujiki, M. *Chem. Lett.* **1999**, 699−700. f. Ichikawa, T.; Yamada, Y.; Kumagai, J.; Fujiki, M. *Chem. Phys. Lett.* **1999**, *306*, 275−279. g. Koe, J. R.; Fujiki, M.; Nakashima, H. *J. Am. Chem. Soc.* **1999**, *121*, 9734−9735. h. Koe, J. R.; Fujiki, M.; Motonaga, M.; Nakashima, H. *Chem. Commun.* **2000**, 389−390. i. Fujiki, M. *J. Am. Chem. Soc.* **2000**, *122*, 3336−3343. j. Toyoda, S.; Fujiki, M. *Macromolecules* **2001**, *34*, 640−644. k. Toyoda, S.; Fujiki, M. *Macromolecules* **2001**, *34*, 2682−2685. m. Fujiki, M.; Koe, J. R.; Motonaga, M.; Nakashima, H.; Terao, K.; Teramoto, A. *J. Am. Chem. Soc.* **2001**, *123*, 6253−6261.

(12) a. Terao, K.; Terao, Y.; Teramoto, A.; Nakamura, N.; Terakawa, I.; Sato, T.; Fujiki, M. *Macromolecules* **2001**, *34*, 2682−2685. b. Terao, K.; Terao, Y.; Teramoto, A.; Nakamura, N.; Fujiki, M.; Sato, T. *Macromolecules* **2001**, *34*, 4519−4525. c. Terao, K.; Terao, Y.; Teramoto, A.; Nakamura, N.; Fujiki, M.; Sato, T. *Macromolecules* **2001**, *34*, 6519−6525. d. Natsume, T.; Wu, L.; Sato, T.; Terao, K.; Teramoto, A.; Fujiki, M. *Macromolecules* **2001**, *34*, 7899−7904.

(13) a. Yashima, E.; Matsushima, T.; Okamoto, Y. *J. Am. Chem. Soc.* **1997**, *119*, 6345−6359. b. Yashima, E.; Maeda, Y.; Okamoto, Y. *J. Am. Chem. Soc.* **1998**, *120*, 8895−8896. c. Yashima, E.; Maeda, K.; Okamoto, Y. *Nature* **1999**, *399*, 449−451.

Table 1. Numerical Results from Light Scattering, Sedimentation Equilibrium, and Viscometry on PRS Samples in Isooctane at 25 °C

sample	$10^{-4}\,M_w$	N_w[c]	A_2[d]	$\langle S^2\rangle_z^{1/2}$[e]	M_z/M_w	$[\eta]$[f]	k'
RS-2	135[a]	5300	3.4[a]	180		48.0	0.38
RS-3	91.4[a]	3590	3.1[a]	143		28.0	0.41
RS-4	26.0[a]	1020	3.0[a]	60		6.38	0.42
RS-5	9.0_5[b]	356	4.3[b]		1.1_8	1.54	0.42
RS-6	3.90[b]	153	4.5[b]		1.1_1	0.465	0.4_5
RS-7	1.81[b]	71.1	7.0[b]		1.0_3		
RS-8	0.89_2[b]	35.0	20[b]		1.1_0		

[a] From light scattering. [b] From sedimentation equilibrium. [c] Calculated by the equation $N_w = M_w/254.5$. [d] In units of 10^{-4}cm^3 mol g^{-2}. [e] In units of nm. [f] In units of 10^{-2}cm^3 g^{-1}.

were determined by analyzing the light scattering data by the established procedure.[12b,c] Table 1 summarizes the values of these molecular parameters along with those for $[\eta]$ and k'; N_w is the weight-average number of Si atoms per molecule defined by $N_w = M_w/M_0$, with M_0 being the molecular weight of a Si unit and calculated to be 254.5 for PRS. All the A_2 values in this table are larger than 3×10^{-4} mol g^{-2} cm^3, and k' is around 0.4, indicating that this polysilylene is *molecularly dispersed in a good solvent, isooctane*. This table also contains the values of M_z/M_w for the four samples determined by sedimentation equilibrium, indicating all the samples are reasonably narrow in molecular weight distribution. The higher molecular weight samples were also found to be narrow by GPC.

Figure 1a shows a double-logarithmic plot of $[\eta]M_0$ versus N_w for PRS in isooctane at 25 °C along with our previous data for PH2MBS at 20 °C and PH3MPS at 25 °C.[12a,b] The data for PRS samples are near to those for PH2MBS and follow a straight line with a slope of 1.3. Figure 1c shows the $\langle S^2\rangle_z^{1/2}$ values for these polysilylenes in the same solvent conditions; the slope of the plot for PRS is about 0.7. Thus, these data are consistent with the viscosity data and suggest that the backbone conformation of PRS is slightly stiffer and much stiffer than those of PH2MBS and PH3MPS, respectively. As shown in Figure 1b, the temperature dependence of $[\eta]$ for RS-3 in isooctane is gradual even around 3 °C, where the helical sense is reversed. Thus, PRS is a nearly rodlike polymer and shows no transition in global properties in the temperature range studied.

UV and CD Spectra and Optical Activity. Figure 2 shows the CD and UV spectra of RS-4 in isooctane at the indicated temperatures (panel a) and those of indicated PRS samples at −30 °C (panel b). It is seen that this sample has a sharp absorption peak centered at 320 nm. On the other hand, the UV absorption spectra for the lower molecular-weight samples become smaller and broader with decreasing M_w. To quantify these features of the spectra, we determined the wavelength (λ_{max}) of the peak, the full width at half-maximum (*fwhm*), and the peak height (ϵ_{max}) from the UV spectra evaluated over a wide temperature range. There was no thermal history observed in these spectra. The N_w dependence of these values in isooctane at −70 °C, 5 °C, and 85 °C is illustrated in Figure 3. It is seen that each plot tends to level off at high N_w, approaching some asymptotic value. The same trend is seen at all temperatures studied. These asymptotic values $\lambda_{max,\infty}$, $fwhm_\infty$, and $\epsilon_{max,\infty}$ are plotted against temperature in Figure 4 along with the data for PH3MPS studied previously.[12c] All the plots are linear, although the change in $\lambda_{max,\infty}$ is much smaller than in the others. The shape of the UV spectrum for PRS becomes broader with rising temperature, but the slopes of the plots for both $fwhm_\infty$ and $\epsilon_{max,\infty}$ are much smaller than those for PH3MPS. Therefore, this suggests that the fluctuation of helical conformation is smaller for PRS than for PH3MPS at the same temperature, and this difference between these two polysilylenes becomes more remarkable with rising temperature.

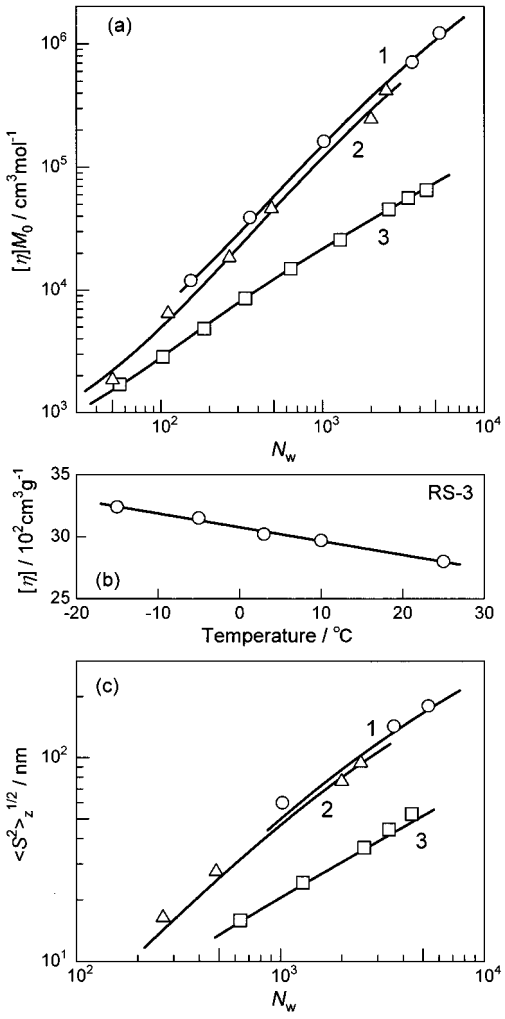

Figure 1. Global properties in isooctane: (a) N_w dependence of $[\eta]M_0$, (b) temperature dependence of $[\eta]$ for RS-3, and (c) N_w dependence of $\langle S^2\rangle_z^{1/2}$. PRS at 25 °C, circles and curve 1; PH2MBS at 20 °C, triangles and curve 2; PH3MPS at 25 °C, squares and curve 3. Curves corresond to theoretical values for PRS ($q = 103$ nm, $d = 3.0$ nm, and $M_L = 1270$ nm^{-1}), PH2MBS ($q = 85$ nm, $d = 2.0$ nm, and $M_L = 934$ nm^{-1}),[12a] and PH3MPS ($q = 6.1$ nm, $d = 1.7$ nm, $B = 1.7$ nm, and $M_L = 1010$ nm^{-1}).[12b] B corresponds to the excluded-volume parameter.[14,18]

It has been shown in our previous paper[12c] that CD and UV spectra of PH3MPS for a given sample at the same temperature are similar in shape, and the Kuhn dissymmetry ratio g_{abs} defined as $g_{abs} \equiv \Delta\epsilon/\epsilon$ could be determined accurately from the ratio of their peak areas. This is also the case with PRS, as seen in Figure 2. Figure 5 shows the temperature dependence of g_{abs} determined in this way for PRS samples. The values of g_{abs} for higher molecular weight samples RS-2 to RS-5 are almost the same, indicating no molecular weight dependence. For these samples, g_{abs} increases with lowering temperature below −30 °C and approaches an asymptotic value of 2.0×10^{-4} at lower temperatures. However, it sharply decreases with rising temperature between −30 °C and 25 °C, passing zero at about 3 °C, and increases at higher temperatures after a minimum. For the low molecular-weight samples, the temperature dependence becomes gentler as the molecular weight is decreased. It is emphasized, however, that the transition temperature, T_c, where g_{abs} becomes zero, is located at about 3 °C independent of samples within experimental errors. This trend resembles closely

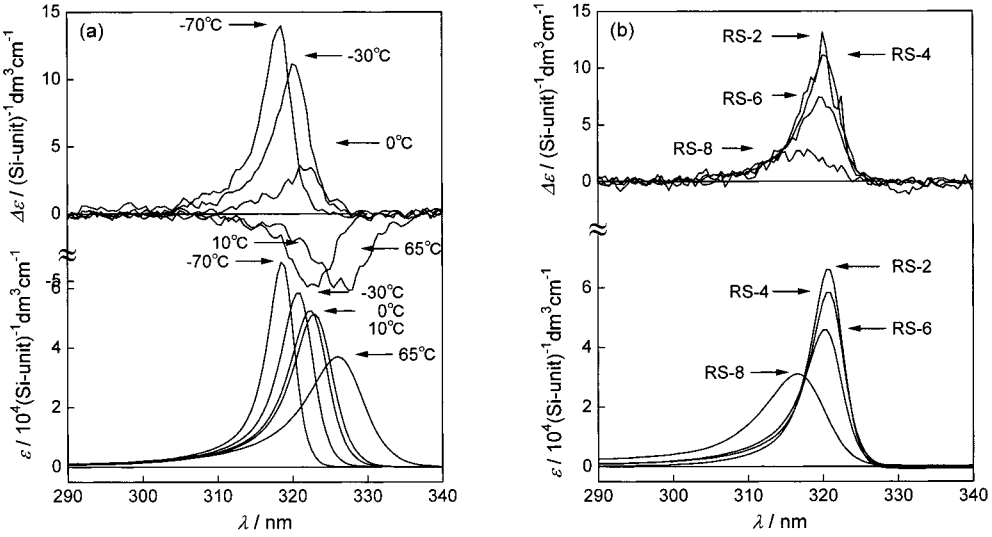

Figure 2. CD and UV absorption spectra in isooctane for (a) sample RS-4 at the indicated temperatures and (b) the indicated PRS samples at −30 °C.

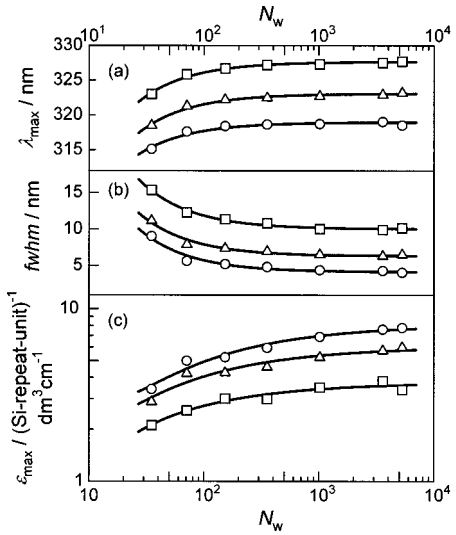

Figure 3. N_w dependence of UV spectra for PRS in isooctane at −70 °C (circles), at 5 °C (triangles), and at 85 °C (squares). Ordinate values: (a) λ_{max}, (b) *fwhm*, and (c) ϵ_{max}.

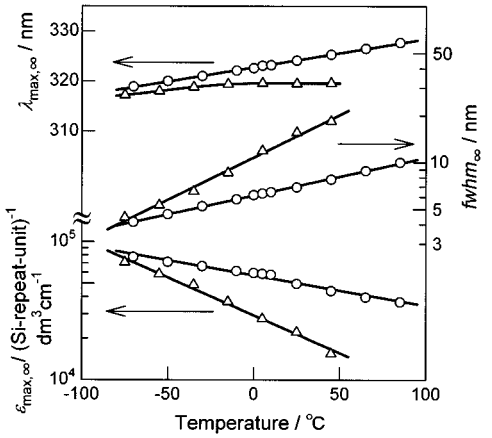

Figure 4. Temperature dependence of UV spectra for PRS (circles) with infinitely large molecular weight. Triangles correspond to reproduced data for PH3MPS.[12c]

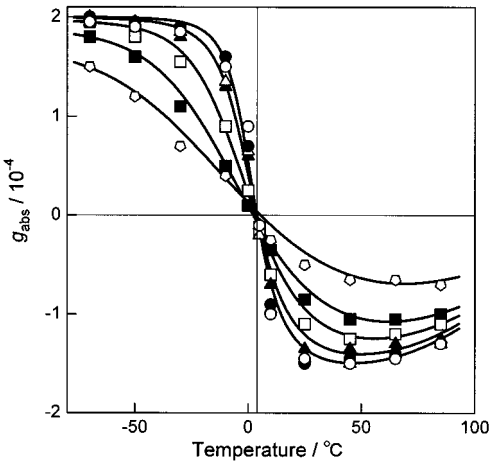

Figure 5. Temperature dependence of g_{abs} for PRS samples in isooctane: unfilled circles, RS-2; filled circles, RS-3; unfilled triangles, RS-4; filled triangles, RS-5; unfilled squares, RS-6; filled squares, RS-7; pentagons, RS-8.

the prediction based on the helix reversal model as will be shown in Figure 7b.

The molecular-weight dependence of g_{abs} at fixed temperature is illustrated in Figure 6. The values of g_{abs} are almost independent of molecular weight in the range $N_w > 10^3$, but their absolute values for lower molecular-weight samples decrease significantly with decreasing N_w. This molecular-weight dependence is a key characteristic in order to discuss ΔG_h and ΔG_r for the helical conformations of PRS in isooctane. It should be noted that solutions of PH3MPS[12c] and polyisocyanates[6c,6e] exhibit similar behavior but have no sign change in optical activity.

Discussion

1. Rodlike Nature of Poly(silylene)s: Stiffness and Electronic Properties. As shown in Figure 1a, $[\eta]$ of PRS changes with a high power of N_w, indicating this to be a stiff-chain polymer; the $M_0[\eta]-N$ relation is rather insensitive to d and determined essentially by q. It is well-established that such a molecular-weight dependence of $[\eta]$ is analyzed by the Yamakawa−Fujii−Yoshizaki theory based on the wormlike-cylinder model,[14,15] which is characterized by the contour length L, the chain diameter d, and the persistence length q of the cylinder; L is related to the molecular weight M by $L = M/M_L$,

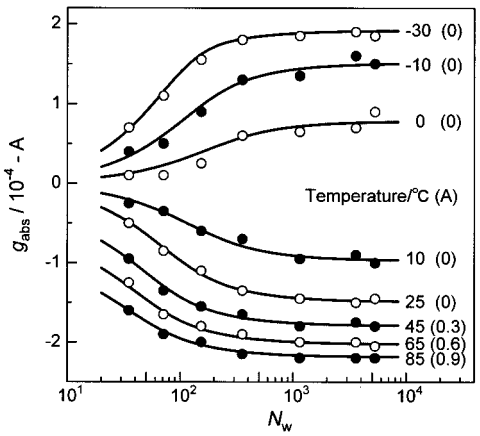

Figure 6. Plots of g_{abs} versus N_w for PRS in isooctane at the indicated temperatures. Solid lines correspond to theoretical values calculated from eq 9 with the parameters presented in Figure 8. For clarity, the ordinate values of g_{abs} are shifted by A in the parentheses.

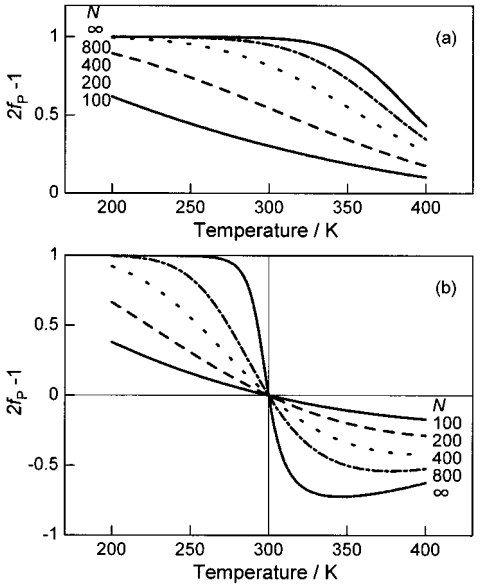

Figure 7. Plots of $2f_P - 1$ versus absolute temperature. Curves are calculated values from the statistical mechanical theory with $\Delta G_r = 2 \times 10^4$ J mol^{-1} and $\Delta G_h = -20\ (1 - T/T_c)$ J mol^{-1}; (a) $T_c = 500$ K, and (b) $T_c = 300$ K.

with M_L being the mass per unit contour length. This theory for the intrinsic viscosity $[\eta]$ of an unperturbed wormlike cylinder can be expressed in a good approximation as

$$(M^2/[\eta])^{1/3} = I + SM^{1/2} \qquad (1)$$

with I and S being known functions of q, M_L, and d.[16,17] This equation is correct in the range $L/2q = 0.4-300$ for typical stiff chains, and a plot of $(M_w 2/[\eta])^{1/3}$ versus $M_w^{1/2}$ should give a straight line with the ordinate intercept I and the slope S which contain q, M_L, and d.

It is shown that the plot of $(M_w 2/[\eta])^{1/3}$ versus $M_w^{1/2}$ constructed from the data for PRS in Table 1 is a straight line as predicted, with the data for the lowest M_w deviating slightly downward. Thus, we have three relations, I, S, and this deviation, for the three wormlike chain parameters to be determined separately, as shown also for PH3MPS.[12b] The best fit values for M_L, q, and d are $M_L = 1270 \pm 50$ nm^{-1}, $q = 103 \pm 10$ nm, and $d = 3.0 \pm 1.0$ nm. It is noted that excluded-volume effects[14,18] on $[\eta]$ and $\langle S^2 \rangle_z$ are shown to be negligible because the value of $M_w/2qM_L$ is 5.2, even for the sample RS-2, having the highest molecular weight in this study. Curve 1 of Figure 1a represents the theoretical values of $[\eta]$ calculated with these parameters and fits the data point accurately. This model is also applied precisely to PH2MBS (curve 2, $q = 85$ nm)[12a] and PH3MPS (curve 3, $q = 6.1$ nm).[12b]

Solid curve 1 in Figure 1c represents the theoretical values of $\langle S^2 \rangle^{1/2}$ calculated by[19]

$$\langle S^2 \rangle = \frac{qM}{3M_L} - q^2 + \frac{2q^2 M_L}{M}\left[1 - \frac{qM_L}{M}(1 - e^{-(M/qM_L)})\right] \qquad (2)$$

for the wormlike chain with $q = 103$ nm and $M_L = 1270$ nm^{-1}. The data points (circles in Figure 1c) are seen to deviate slightly upward from the curve, but the deviation is in the range estimated from the polydispersity of these samples. The helix pitch per Si unit is calculated from the estimated M_L value to be 0.20_0 nm. This value is consistent with the value of a 7_3 helix, that is, 0.197 nm, for poly(di-*n*-pentyl silylene) and poly(di-*n*-butyl silylene) in the crystal state.[9,20] On the other hand, $q = 103$ nm for PRS is the highest among all the polysilylenes to our knowledge, that is, PH2MBS ($q = 85$ nm),[12a] PH3MPS ($q = 6.1$ nm),[12b] and poly(di-*n*-hexylsilylene) ($q = 3$ nm)[21] around room temperature.

As far as their global conformations are concerned, the polysilylenes investigated so far can be regarded as continuous wormlike cylinders characterized by the persistence length q. In principle, q is determined by the fluctuations in local conformations, which are related to their electronic properties, such as λ_{max}, ϵ_{max}, and *fwhm*. Elucidation of such correlations may be a theoretical challenge.

2. Cooperative Transition. A. Theoretical framework. It has been shown in our previous paper[12c] that a chiro-optical property of PH3MPS depends remarkably on temperature and molecular weight. This behavior is very similar to those of chiral polyisocyanates studied by Teramoto, Green, and collaborators.[6] For the polyisocyanates, the backbone chain conformation consists of the M and P helices, but the helix sense depends on the side chain, solvent, and temperature; M or P may be either left-handed or right-handed. Lifson et al.[6a] developed a statistical mechanical theory using a helix reversal model, where a given chain consists of an alternating sequence of the two helices intervened by helix reversals. Assuming that the two helices are nearly symmetric, the optical activity detected by CD or OR (optical rotation) of the polymer solution arises from the excess presence of one helix. The theory is characterized by the three statistical parameters u_M, u_P, and u_r, or associated free energies, G_M, G_P, and G_r, where the subscripts M, P, and R represent the quantities associated with the M and P helical units and helix reversal units, respectively. Without loss of generality, they are reduced to two energy functions $\Delta G_r \equiv G_r - (1/2)(G_M + G_P)$ and $2\Delta G_h \equiv G_M - G_P$ and related to statistical weights u_M, u_P, and u_r by

(14) Yamakawa, H. *Helical Wormlike Chains in Polymer Solutions*; Springer: Berlin, 1997.
(15) a. Yamakawa, H.; Fujii, M. *Macromolecules* **1974**, *7*, 128−135. b. Yamakawa, H.; Yoshizaki, T. *Macromolecules* **1980**, *13*, 633−643.
(16) Bushin, S. V.; Tsvetkov, V. N.; Lysenko, E. B.; Emelyanov, V. N. *Vyskomol. Soedin., Ser. A* **1981**, *A23*, 2494.
(17) Bohdanecký, M. *Macromolecules* **1983**, *16*, 1483−1492.
(18) a. Norisuye, T. *Prog. Polym. Sci.* **1993**, *18*, 543−584. b. Norisuye, T.; Tsuboi, A.; Teramoto, A. *Polym. J.* **1996**, *28*, 357−361.
(19) Benoit, H.; Doty, P. *J. Phys. Chem.* **1953**, *57*, 958.
(20) Miller, R. D.; Farmer, B. L.; Fleming, W.; Sooriyakumaran, R.; Rabolt, J. *J. Am. Chem. Soc.* **1987**, *109*, 2509−2510.
(21) Cotts, P. M. *Macromolecules* **1994**, *27*, 2899−2903.

$$u_M = \exp(-\Delta G_h/RT) \quad u_P = \exp(+\Delta G_h/RT)$$
$$u_r = v = \exp(-\Delta G_r/RT) \quad (3)$$

This theory is shown to describe the molecular weight dependence of OR quantitatively not only for homopolyisocyanates but also for copolymers of chiral and achiral isocyanates.[6] They belong to typical linear cooperative systems, or Ising systems, also including α-polypeptides. Selinger et al.[22] treated copolyisocyanates from a different approach, showing that a minute excess in chirality brings about remarkable optical activity. Recently, a general theoretical framework[1] has been given to treat such typical linear cooperative systems, pointing out the importance of the conformations of terminal units, whether they are restricted in specific ones or not. This restriction is described by the components of the terminal vectors, *a* and *b*, and the partition function of this polymer chain is given by[1]

$$Z_N = \mathbf{A}\mathbf{M}^{N-1}\mathbf{B} \quad (4)$$

where **M** is the statistical weight matrix defined by

$$\mathbf{M} = \begin{pmatrix} u_M & v u_P \\ v u_M & u_P \end{pmatrix} \quad (5)$$

and

$$\mathbf{A} = (a u_M \;\; u_P) \quad \mathbf{B} = \begin{pmatrix} b \\ 1 \end{pmatrix} \quad (6)$$

There is no restriction for $a = b = 1$.

The average conformation of a polymer chain is described by the fraction f_P of monomer units in the P helical conformation and optical activity $2f_P - 1$ is obtained from Z_N by the standard procedure in statistical mechanics as

$$f_P = (1/N)\frac{\partial(\ln Z_N)}{\partial(\ln u_P)} \quad (7)$$

and the number of helix reversals per chain n_r is given by

$$n_r = \frac{\partial(\ln Z_N)}{\partial(\ln v)} \quad (8)$$

Lifson et al.[6a] have derived $2f_P - 1$ and n_r from a different approach, which agree with eqs 7 and 8, respectively, but are inaccurate at smaller values of *N*.

Figure 7 illustrates some theoretical calculations for the helix reversal model for the case $a = b = 1$, that is, no restriction on the end units. Panel a shows $2f_P - 1$ plotted against temperature at fixed ΔG_r and slightly temperature dependent $\Delta G_h = -20(1 - T/T_c)$ J mol^{-1}; $T_c = 500$ K. It is seen that $2f_P - 1$ decreases monotonically with temperature for each *N* and tends to vanish at higher temperature, and at a fixed temperature, $2f_P - 1$ increases with *N*, approaching an asymptotic limit at infinite *N*. This is the behavior observed for chiral polyisocyanates.[6e,f,g] Panel b illustrates the thermal transition curves with no terminal restriction, but T_c is located at 300 K. It is seen that for large *N*, $2f_P - 1$ now drops very sharply around 300 K, changes its sign at T_c, and passes through a shallow minimum to higher temperature. At any temperature, $2f_P - 1$ is predicted to change with *N*. This behavior is essentially the same as the experimental

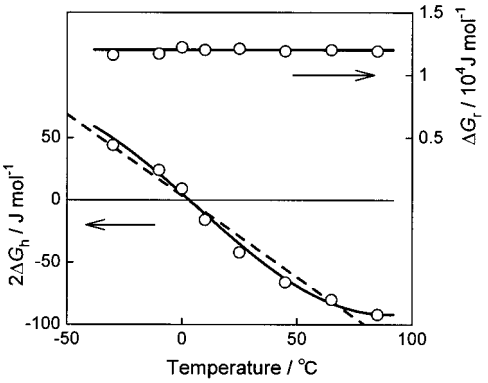

Figure 8. Temperature dependences of $2\Delta G_h$ and ΔG_r in isooctane. Solid curve, ΔG_h calculated by eq 10; dashed curve, ΔG_h calculated by eq 15 with $\Delta\phi_{MP} = 1.17$ and $\Delta E_{MP} = 360$ J mol^{-1}.

results shown in Figures 5 and 6. It can be shown that the transition becomes very sharp as *v* tends to vanish, but a first-order transition is not expected unless $v/N = 0$. Thus, Schweizer's claim[23] that a conjugating polymer would undergo a *first-order* helix−coil transition is not rationalized. Toriumi[24] discussed a left-handed to-right-handed helix transition with a special reference to polyaspartate derivatives; this is a special case with random coil units for helix reversal units.

B. Analysis of Experimental Data. Next, we try to analyze these results using the described theory without terminal restriction. First, the observed g_{abs} data are converted to f_P in the following way. Assuming that the M and P helices have the same absolute value of g_{abs} per monomer unit, g_m, the theoretical f_P can be related to g_{abs} by

$$\frac{n_P - n_M}{n_P + n_M} = 2f_P - 1 = \frac{g_{abs}}{g_m} \quad (9)$$

It is noted that UV and CD spectra are similar in shape, although their strengths change largely with molecular weight and temperature. This strongly supports the validity of the above assumption.[11b] The theory can be tested by fitting the experimental data for f_P as a function of *N* at a fixed temperature. If the fitting is successful, the theory is validated, and the fitting parameters, $v(T)$ and $\Delta G_h(T)$, are determined at that temperature with no assumption on their *T* dependence.

Assuming a value of 2×10^{-4} for g_m, which is the asymptotic value of g_{abs} for PRS in isooctane, trial-and-error procedures were repeated to have the best fit. The solid curves in Figure 6 represent the theoretical values calculated for the best-fit parameters, which follow the data points closely, justifying our starting assumption. Figure 8 shows how these parameters change with *T*. It is seen that $\Delta G_r(T)$ stays at 1.2×10^{-4} J mol^{-1}, whereas $\Delta G_h(T)$ changes sigmoidally with *T*, passing through zero at 3 °C. This change in $\Delta G_h(T)$ explains the steep change in $2f_P - 1$ around T_c, whose molecular-weight independence is the consequence from $a = b = 1$. The change in $\Delta G_h(T)$ with *T* is expressed by eq 10 (the solid curve in Figure 8):

$$\Delta G_h = -3 + 43\sin[-0.019(T/\mathrm{K} - 280)] \text{ (J mol}^{-1}) \quad (10)$$

It can be shown that the g_{abs} for all the samples in the entire temperature range studied are fitted precisely by the theoretical

(22) a. Selinger, J. V.; Selinger, R. L. B. *Phys. Rev. E* **1997**, *55*, 1728−1731. b. Selinger, J. V.; Selinger, R. L. B. *Phys. Rev. Lett.* **1996**, *76*, 58−61.

(23) a. Schweizer, K. S. *J. Chem. Phys.* **1986**, *85*, 1156−1175. b. Schweizer, K. S. *J. Chem. Phys.* **1986**, *85*, 1176−1183.

(24) Toriumi, H. *Macromolecules* **1984**, *17*, 1599−1605.

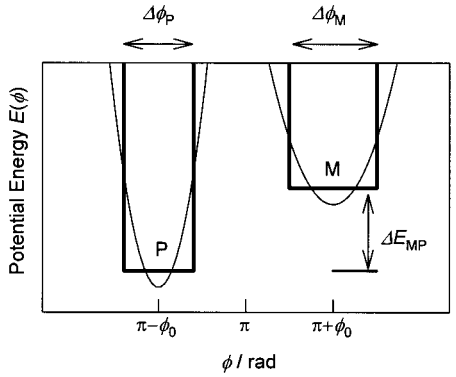

Figure 9. Schematic representation of a double-well potential.

curves with eq 10, $g_m = 2 \times 10^{-4}$, and $\Delta G_r(T) = 1.2 \times 10^4$ J mol^{-1}.

To be more precise, g_m may change with temperature because $\lambda_{max,\infty}$ changes with temperature (see Figure 4). Previously,[11m] we estimated g_m from $g_{abs,\infty}$ values for poly{[(*S*)-3,7-dimethyloctyl]-[2-methylpropyl]}silylene (rigid polysilylene) as

$$g_{abs,\infty} = 2.28 \times 10^{-4} - 3.2 \times 10^{-7}(T/\mathrm{K} - 273.15) \quad (11)$$

The $g_{abs,\infty}$ value calculated by this equation changes from 2.55×10^{-4} at −85 °C to 2.0×10^{-4} at 85 °C. However, the free energy parameters estimated using this equation are equal to those for a constant value of 2.0×10^{-4}, except those at −30 °C.

C. Double-Well Potential and Solvent Effect. We have proposed a double-well potential in order to account for the temperature change of $2f_P - 1$ or $\Delta G_h(T)$.[11m] We try to correlate this proposal to the present theoretical analysis. Suppose a double-well potential for the rotation ϕ about the main-chain Si−Si bond, where the two energy minima for the M and P helices are located at $\phi_M = \pi + \phi_0$ and $\phi_P = \pi - \phi_0$, respectively, and the energy minimum for the P helix is deeper and steeper than that for the M helix, as schematically shown in Figure 9. The statistical weights u_M and u_P are given by

$$u_M = \int_M \exp[-E(\phi)/RT]\, d\phi \quad u_P = \int_P \exp[-E(\phi)/RT]\, d\phi \quad (12)$$

If each energy minimum is approximated by a square well of the depth E_M (or E_P) and width $\Delta\phi_M$ (or $\Delta\phi_P$), these equations are simplified to give

$$u_M(T) = \Delta\phi_M \exp[-E_M/RT] \quad u_P(T) = \Delta\phi_P \exp[-E_P/RT] \quad (13)$$

and the ratio u_M/u_P is

$$\frac{u_M(T)}{u_P(T)} = \left(\frac{\Delta\phi_M}{\Delta\phi_P}\right) \exp\left[\frac{-(E_M - E_P)}{RT}\right] = \Delta\phi_{MP} \exp\left[\frac{-\Delta E_{MP}}{RT}\right] = \exp\left[\frac{-2\Delta G_h(T)}{RT}\right] \quad (14)$$

with

$$\Delta E_{MP} = E_M - E_P \qquad \Delta\phi_{MP} = \Delta\phi_M/\Delta\phi_P$$
$$2\Delta G_h(T) = \Delta E_{MP} - RT \ln(\Delta\phi_{MP}) \quad (15)$$

This equation predicts that $2f_P - 1$ approaches unity as T goes to zero, but remains between 0 and −1 as T goes to infinity, if both ΔE_{MP} and $\ln(\Delta\phi_{MP})$ are positive. The dashed line in Figure 8 represents the theoretical values calculated by eq 14 with $\Delta\phi_{MP} = 1.17$ and $\Delta E_{MP} = 360$ J mol^{-1}. The theoretical line follows the data points almost quantitatively. Thus, we see that the dissymmetry between the M and P helical conformations is significant both in the energetic and entropic aspects because of the large chiral side chains. This is contrasted with PH3MPS, which is characterized by small ΔG_h only monotonically changing with temperature. This polymer has only one chiral side chain, (*S*)-3-methylpentyl, and hence, its helical conformations are much more symmetric than those of PRS; at higher temperature, ΔE_{MP} is about 50 J mol^{-1}, $\Delta\phi_{MP} = 1.017$, and T_c may be located far above room temperature. Although some calculations of the potential are available,[11m] they are not accurate enough to predict the values of ΔE_{MP} and $\Delta\phi_{MP}$ estimated previously for PRS and PH3MPS.

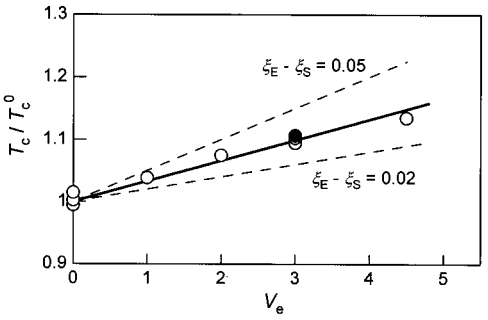

Figure 10. Plots of T_c/T_c^0 against V_e: ●, present data; ○, previous data;[11m] solid line calculated by eq 17 with $\xi_E - \xi_S = 0.033$.

It is assumed in the above analysis that the three parameters, ΔE_{MP}, $\Delta\phi_{MP}$, and ΔG_r, are independent of temperature. This may be a reasonable approximation, unless T is much removed from T_c. Thus, the working hypothesis of the three regions proposed previously[11m] may be justified for large N but is not necessarily needed.

It is shown in our previous publication[11m] that T_c depends remarkably on solvent. Next, we will incorporate this solvent effect into eq 14. We assume that in a given solvent the energy and entropy terms in eq 14 increase by small fractions $\xi_E V_e$ and $\xi_S V_e$ respectively, where V_e is a volume variable and ξ_E and ξ_s are the corresponding interaction parameters. This implies that the corresponding terms in eq 14 should be rewritten

$$\Delta E_{MP}(T) \rightarrow (1 + \xi_E V_e)\Delta E_{MP}(T)$$
$$\ln(\Delta\phi_{MP}) \rightarrow (1 + \xi_S V_e)\ln(\Delta\phi_{MP}) \quad (16)$$

and the transition temperature without and with solvent interaction, T_c° and T_c are related by

$$\frac{T_c}{T_c^\circ} = \frac{1 + \xi_E V_e}{1 + \xi_S V_e} \cong 1 + (\xi_E - \xi_S)V_e \quad (17)$$

This equation predicts that the energy increase raises T_c, whereas the entropy increase lowers T_c, and T_c increases linearly with V_e if ξ_E, ξ_s, and $\xi_E - \xi_s$ are positive. Physically, this dictates the situation that smaller solvent molecules penetrate freely into the helical cavity formed by the side chains, whereas the larger ones do not, and the cavity is in turn compressed and loses freedom. Thus, the larger V_e brings about the larger T_c change. Figure 10 shows some theoretical calculations of T_c as a function

of V_e for this model; V_e is taken to be the number of branches based on C5 chains.[11m] It is seen that T_c increases nearly linearly with V_e more remarkably with stronger interaction. This trend is in harmony with the solvent dependence of T_c found by Fujiki et al.,[11m] and eq 17 with $\xi_E - \xi_s = 0.033$ (solid line) reproduces the present and their T_c data correctly. It is interesting to apply this idea to other conjugating polymers undergoing similar conformational transitions. In this paper, we have not mentioned an interesting correlation between conformational characteristics and global properties. This will be discussed in a forthcoming paper.[25]

(25) Sato, T.; Terao, K.; Teramoto, A. *Macromolecules*, submitted.

Acknowledgment. A.T. thanks Yamashita Sekkei, Ltd. for the chair professorship at Ritsumeikan University and Professor Mark M. Green of Polytechnic University for drawing his attention to polysilylenes. The authors thank Dr. Hiroshi Nakashima, Professor Julian R. Koe, and Dr. Masao Motonaga for their fruitful discussions. M.F. is also grateful to Drs. Keiichi Torimitsu and Hideaki Takayanagi for their generous support.

Supporting Information Available: Details of experimental methods and data treatments and values of $[\eta]$, *fwhm*, ϵ_{max}, λ_{max}, g_{abs}, ΔG_h, and ΔG_r (PDF). This material is available free of charge via the Internet at http://pubs.acs.org.

JA011550F